Cell. Mol. Life Sci. (2010) 67:1491–1503
DOI 10.1007/s00018-010-0262-5

Cellular and Molecular Life Sciences

RESEARCH ARTICLE

Deimination is regulated at multiple levels including auto-deimination of peptidylarginine deiminases

Marie-Claire Méchin · Fanny Coudane · Véronique Adoue · Jacques Arnaud · Hélène Duplan · Marie Charveron · Anne-Marie Schmitt · Hidenari Takahara · Guy Serre · Michel Simon

Received: 3 September 2009 / Revised: 1 December 2009 / Accepted: 7 January 2010 / Published online: 29 January 2010

Abstract Peptidylarginine deiminases (PADs) catalyze deimination, converting arginyl to citrullyl residues. Only three PAD isotypes are detected in the epidermis where they play a crucial role, targeting filaggrin, a key actor for the tissue hydration and barrier functions. Their expression and activation depends on the keratinocyte differentiation state. To investigate this regulation, we used primary keratinocytes induced to differentiate either by increasing cell-density or by treatment with vitamin D. High cell-density increased PAD1 and 3, but not PAD2, at the mRNA and protein levels, and up-regulated protein deimination. By contrast, vitamin D increased PAD1–3 mRNA amounts, with distinct kinetics, but neither the proteins nor the deimination rate. Furthermore, auto-deimination was shown to decrease PAD activity, increasing the distances between the four major amino acids of the active site. In summary, deimination can be regulated at multiple levels: transcription of the *PADI* genes, translation of the corresponding mRNAs, and auto-deimination of PADs.

Keywords Post-translational modification · Keratinocyte · Differentiation · Citrulline · Arginine · Calcium · Protein structure

Electronic supplementary material The online version of this article (doi:10.1007/s00018-010-0262-5) contains supplementary material, which is available to authorized users.

M.-C. Méchin · F. Coudane · V. Adoue · J. Arnaud · G. Serre · M. Simon (✉)
CNRS-University of Toulouse III, UMR5165, Institut Fédératif de Recherche 150 (INSERM-CNRS-Université paul Sabatier-Centre Hospitalier Universitaire de Toulouse), CHU Purpan, Place du Dr Baylac TSA40031, 31059 Toulouse Cedex 9, France
e-mail: Michel.Simon@udear.cnrs.fr

H. Duplan · M. Charveron · A.-M. Schmitt
Centre Européen de Recherche sur la Peau et les Epithéliums de Revêtement (CERPER), Pierre Fabre Dermo-Cosmétique, Toulouse, France

H. Takahara
Department of Applied Biological Resource Sciences, School of Agriculture, University of Ibaraki, Ibaraki, Japan

Introduction

In the epidermis, keratinocytes coexist in several states of differentiation to maintain the homeostasis of the tissue so as to assure its vital barrier function, i.e. to protect the whole body against physical, chemical or biological insults. Keratinocytes, characterized by a scarce cytoplasm and a large nucleus, proliferate in the *stratum basale*. They differentiate during their migration to the surface of the stratified tissue and become first spinous cells forming the *stratum spinosum*, then granular keratinocytes in the *stratum granulosum* before finally dying in a unique cell-death program. The resulting cells, called corneocytes, devoid of nucleus and other organelles, accumulate in the *stratum corneum* and are finally eliminated at the skin surface by the desquamation process. This complex program of differentiation involves structural proteins [(pro)filaggrin, involucrin, keratins, etc.], lipid metabolism enzymes (phospholipases, glucocerebrosidases, etc.) and post-translational modification enzymes, including proteases (kallikreins, cathepsins, etc.), transglutaminases, and peptidylarginine deiminases (PADs).

PADs (E.C. 3.5.3.15) have been detected in most organs, tissues, and cells. They catalyze the deimination (or citrullination) reaction in the presence of calcium, converting arginyl residues into citrullyl residues (for a recent review, see [1]). They are suspected to be involved in the

pathological events of several severe human diseases such as multiple sclerosis and rheumatoid arthritis (reviewed in [1–4]). In the skin, the main PAD targets are filaggrin and keratins K1 and K10 in the epidermis [5], and trichohyalin in the hair follicles [6]. Deimination induces charge loss on the targeted protein and changes its conformation, its interactions (either association or dissociation), and therefore its function, as has been well documented for trichohyalin [7, 8] and recently for S100A3 [9].

Filaggrin deimination could induce its dissociation from intermediate filaments and its subsequent degradation to free amino acids, producing the so-called natural moisturizing factor, important for the epidermal barrier functions as it retains water in the *stratum corneum* and adsorbs part of UV radiation [1, 10]. Importantly, a reduced amount of filaggrin, which is associated with reduced levels of hygroscopic amino acids and altered barrier functions, underlies ichthyosis vulgaris (OMIM 146700) and is a major risk factor for atopic dermatitis (OMIM 603165), two very common skin diseases often associated with rhinitis and asthma. The known reasons for filaggrin decrease are profilaggrin-gene null mutations [11–13] and cytokine-induced down-regulation [14, 15]. Defective PAD activities can also be suspected since in vitro deimination of filaggrin increases its proteolysis by calpain I and bleomycin-hydrolase, two proteases involved in its processing in the lower *stratum corneum* [16]. Therefore, a default of PAD activity could disturb filaggrin metabolism and natural moisturizing factor production, and consequently the epidermal barrier function efficiency. Moreover, decreased levels of deimination have been observed in patients with bullous congenital ichthyosiform erythroderma (OMIM 113800) and psoriasis (OMIM 177900) [17, 18]. It is therefore of major importance to know how PADs and deimination are regulated during keratinocyte differentiation.

There are five PADs (PAD1–4 and 6), encoded by distinct genes (*PADI*1–4 and 6) clustered in a single locus at 1p35–36 [19]. In the epidermis, PAD1 has been immunodetected throughout the tissue, PAD2 in the suprabasal living keratinocytes, and PAD3 in the granular keratinocytes and in the deeper corneocytes, whereas *PADI*4 and 6 are not expressed [20–23]. Using cultures of primary normal human keratinocytes (NHKs) induced to differentiate by a shift of calcium concentration in the medium, we have previously shown that this pattern of expression is due in part to regulation of *PADI* gene expression at the transcriptional level ([24–28]; see also, for a recent review [29]).

In the present work, to more precisely analyze the regulation of PADs and deimination, we successively developed two other well-known models of in vitro NHK differentiation. In these models, NHK differentiation was induced (1) by addition, in a defined culture medium, of the active form of vitamin D (Vit D), the 1-α, 25-dihydroxyvitamin D3 [30–34], and (2) by increasing the cell density [35–37]. Since PADs seem to be regulated not only at the transcriptional but also at the translational and post-translational levels in other cell types [38, 39], we tested the effect of differentiation of NHKs on the steady-state levels of *PADI* mRNAs, and also on PAD1–3 protein amounts and on PAD activity. Moreover, we observed that in vitro PADs can auto-deiminate themselves, the enzymes becoming less active after deimination. Therefore, auto-deimination could be an additional step of regulation in the control of PAD activity.

Materials and methods

Primary keratinocyte cell cultures

To produce primary NHKs, foreskin biopsies were harvested from young children without any history of skin diseases after informed consent had been given by their families according to the ethical guidelines of the University of Toulouse III, the French Ministry of the Research and Technology, and the Declaration of Helsinki. Epidermal keratinocytes were isolated according to the procedure described in [40], and cultured in the defined KBM-2 medium (Promocell, Heidelberg, Germany) supplemented with several growth factors as follows: 0.4% bovine pituitary extract, 0.125 ng/ml epidermal growth factor, 5 μg/ml human insulin, 0.33 μg/ml hydrocortisone, 10 μg/ml human transferrin, 0.39 μg/ml epinephrine, and 0.15 mM $CaCl_2$ in the presence of 100 μg/ml primocin^{TM} (Cayla-Invivogen, Toulouse, France) in a humidified incubator at 37°C with 5% CO_2. The medium was changed every 3 days. When NHKs reached confluence, they were transferred, after a short trypsin incubation, into either 24-well plates at 10^4 cells per well (for RNA extractions) or T25 flasks at 2×10^5 cells per flask (for protein extractions). When the subcultures reached about 70% confluence, NHKs were treated once with either 10^{-7} M Vit D (Sigma-Aldrich, St Louis), 10^{-7} M Vit D and 1.5 mM $CaCl_2$ (Vit D + Ca^{2+}), or 0.1% DMSO (vehicle control), for no longer than 3 days. NHKs were harvested at 6 h, 24 h, 7 days, and 10 days after the start of the treatment. When cell density was used as a differentiation procedure, NHKs were harvested at low (cells covering less than 50% of the surface), intermediate (cells covering 50–70% of the surface), and high (cells covering more than 70% of the surface with a beginning of stratification) cell density, as previously described [41]. In all cases, NHKs were thoroughly washed in PBS after harvesting.

Protein and RNA extractions

For protein extractions, NHKs were homogenized by pipetting into TE-NP40 buffer [50 mM Tris–HCl pH 7.4, 150 mM NaCl, 1% NP-40, 10 mM EDTA and a 1/100 (v/v) cocktail of mammalian protease inhibitors (Sigma-Aldrich)] and shaking for 20 min at 4°C. After centrifugation at 15,000*g* for 20 min at 4°C, soluble proteins in the supernatants were harvested to obtain the "TE-NP40 extracts", conditions known to enable the extraction of all PAD isotypes from different cell types and tissues [22, 38, 42, 43]. The pellets were then solubilized in Laemmli buffer (50 mM Tris–HCl pH 6.8, 0.1% SDS, 1.6% β-Mercapto-ethanol, 0.8% Glycerol, 0.006% Bromophenol-blue) and sonicated on ice (twice, 15 s each) to obtain the "Laemmli extracts" and look for deiminated proteins. Proteins of the "TE-NP40 extracts" were quantified by the Bradford method (Amresco) with a standard BSA curve. After gel electrophoresis and electro-transfer, amounts of protein in the "Laemmli extracts" were estimated by Ponceau S staining. All extracts were stored at −80°C.

For total RNA extractions, NHKs from three wells were homogenized by pipetting with 350 µl of RLT buffer from the RNeasy extraction kit (Qiagen, Courtaboeuf, France), quickly frozen in liquid nitrogen, and stored at −80°C until complete extraction as mentioned in the manufacturer's instructions. A DNase I, RNase free treatment (Qiagen) was performed directly on the column for 15 min at room temperature. Quantity and quality of the RNA were checked with an RNA 6000 nano assay kit using the Agilent 2100 bioanalyzer, according to the manufacturer's instructions (Agilent Technologies, Waldbronn, Germany).

Antibodies and purified recombinant human PAD1–3 and His-filaggrin

The anti-modified-citrulline antibody (AMC) (a generous gift from T. Senshu, Tokyo, Japan) was used at 0.184 µg/ml and the immunodetection was performed as previously described [44]. Anti-PAD antipeptides were produced, purified, and used as previously described [20, 22]. The hPAD2-2110 anti-PAD2 monoclonal antibody, a kind gift from A. Ishigami, Chiba, Japan, was diluted at 1/1,000 as previously described [45]. Its specificity was controlled by western blotting using skin extracts of Pad2 knock-out compared to wild-type mice (Coudane et al., submitted manuscript). Anti-actin monoclonal antibody (MAB1501) was diluted at 1/30,000 (Chemicon International, Southampton, UK). Anti-involucrin monoclonal antibody (clone SY5) was diluted at 1/5,000 (Sigma–Aldrich). The monoclonal antibody AHF11, reacting mainly with deiminated filaggrin, was used at 0.4 µg/ml as previously described [23]. Anti-rabbit and anti-mouse IgG secondary antibodies (Zymed; Clinisciences, Montrouge, France) were diluted at 1/10,000 and 1/8,000, respectively, and used as previously described [20, 22]. Active recombinant human PAD1–3 and His-filaggrin were produced and purified as previously described [23, 46, 47].

Anti-modified citrulline antibody sensitivity and specificity

To test the sensitivity of the AMC antibody, we analyzed by western blotting serial dilutions of a known amount of the deiminated filaggrin subunit. We observed that 100 pg was clearly detectable. Since filaggrin contains 11% of arginine and considering that all are deiminated, this corresponds to a sensitivity of at least 30 fmoles of citrulline. We also observed that synthetic peptides containing only one citrulline could be detected by dot-blot. Three peptides of 14 amino acids, derived from human filaggrin (ESSRDGS**R**HPRSHD, EQSADSS**R**HSGSGH and TGSSTGG**R**QGSHHE), and the corresponding mono-citrullinated peptides (ESSRDGS**Cit**HPRSHD, EQSADSS**Cit**HSGSGH and TGSSTGG**Cit**QGSHHE) were covalently link to biotin by their N-terminal end and purified as previously described [48], incubated with a large excess of neutravidin (Pierce, Rockford, IL) for 1 h at 20°C, and spotted on a nitrocellulose membrane with a dot-blot apparatus (HybriDot®; Whatman-Biometra, Goettingen, Germany). All three mono-citrullinated peptides but none of the corresponding arginine-containing peptides were detected by the AMC antibody, after immunoblotting performed as described above, showing the specificity and sensitivity of the antibody.

Western blotting analysis

Equal amounts of proteins (30 µg; according to Ponceau S red staining) were resolved by 10% sodium dodecylsulfate-polyacrylamide gel electrophoresis (SDS-PAGE) and then electro-transferred to nitrocellulose membranes for western blotting analysis as previously described [20, 22, 44]. Immunoreactivities were quantified in arbitrary units with the ImageJ program available at the following address [http://rsb.info.nih.gov/ij/]. Data were normalized with detection of the housekeeping gene product, actin.

Reverse transcription and real time PCR

For real time PCR, cDNAs were produced in 20 µl from 1 µg of total RNA, with 15 U of AMV reverse transcriptase (RT) from the reverse transcription system kit (Promega, Charbonnières-les-bains, France) and a mixture of 5 mM $MgCl_2$, 1 mM dNTP, 4 mM RecRNasineRibon inhibitor, and 25 ng/µl oligo-dT. First, RNAs were

denatured for 2 min at 70°C, reverse transcribed for 60 min at 42°C, and ultimately denatured for 1 min at 99°C. Each RT product was used for real time PCR after 1/10 dilution and analyzed in duplicate PCR plates. All samples that were to be compared were analysed in the same PCR plates for the genes of interest and the three housekeeping genes used for normalization (*YWHAZ*, *B2M*, and *GAPDH*; Table 1). PCR reactions were performed twice on a Biorad iCycler 96-well block, with the real-time detection system software, V3.0, in 26 µl using iQ sybergreen mixture (Biorad, Marne-la-Coquette, France), each primer at 460 nM (Table 1), and 5 µl of the diluted cDNA with a program as follows: (95°C, 30 s) 3 cycles, (95°C, 1 min 30 s) 1 cycle, (95°C, 15 s; 60°C, 30 s) 40 cycles, (95°C, 1 min 30 s) 1 cycle and (95–20°C, 10 s) 80 steps. For *PADI* genes, several primers were designed with the Beacon Designer or Primer3 software (iQBiorad Beacon designer; http://fokker.wi.mit.edu/primer3/) [49], checked in silico by a "blast" analysis and controlled on positive diluted cDNAs (1/10, 1/30, 1/90, 1/270, 1/810) (Table 1). The efficiencies of the *PADI* primer pairs were determined between 99.5 and 113.5% with cDNAs produced from NHKs, HaCaT cells, and testis (the latter was from the human Multiple Tissue cDNA panel; BD Bioscience, Erembodegen, Belgium). Furthermore, to be sure of *PADI* primer specificities, amplicons were controlled on 2.5% agarose gel, then purified and sequenced. The cycle threshold (Ct) number was defined as an arbitrary number of PCR cycles in which the PCR curves were in the linear range. The Ct values measured for the *PADI* genes and for the differentiation marker genes were normalized to the Ct values of three housekeeping genes according to the function $2^{-\Delta\Delta Ct}$. As previously advised [50], the Ct variations obtained for the three housekeeping genes in the different cell culture conditions were controlled (the ΔCt (mean ± SEM) for *YWHAZ*, *B2M*, and *GAPDH*, were 0.633 ± 0.036, 0.577 ± 0.070, and 0.424 ± 0.204, respectively). In this work, all the reported data correspond to normalization using *YWHAZ*. Similar results were obtained using *B2M* or *GAPDH* (data not shown).

Table 1 Characteristics of primers for Q-PCR experiments

Sequences[a]	Exon or AN[b]	Amplicon size (bp)	Tm (°C)
Genes encoding PADs			
*PADI*1			
agagtgacatcgtggacattc	15	231	86
gctcgtggtaggacaagtagtc	16		
*PADI*2			
ggtgggatgagcagcaagcgaatc	14	165	86
gaacagagcgggcaggtcaatgatg	15		
*PADI*3			
gcagagtgtgacatcattgacatcc	15	173	87
gaccgcaccttctcctccag	16		
*PADI*4			
ccacacggggcaaactgtc	6	170	87
cagcagggagatggtgaggg	7		
*PADI*6			
cgtggagaagtgcattcacctgaac	14	152	86
gcctcgcaaaggacctcttggg	15		
Differentiation marker genes			
FLG			
gcaaggtcaagtccaggagaa	NM_002016	122	85
ccctcggtttccactgtctc			
IVL			
gccaggtccaagacattcaac	NM_005547	110	86
gggtggttatttatgtttgggtgg			
*KRT*10			
tgatgtgaatgtggaaatgaatgc	NM_000421	147	83
gtagtcagttccttgctcttttca			
*LGALS*7			
ctggcacggtgctgagaat	NM_002307	149	88
cttgctgttgaagaccacctc			
House keeping genes			
YWHAZ			
acttttggtacattgtggcttcaa	NM_003406	94	82
ccgccaggacaaaccagtat			
B2M			
acccccactgaaaaagatga	NM_004048	114	83
atcttcaaacctccatgatg			
GAPDH			
tgcaccaccaactgcttagc	NM_002046	87	84
ggcatggactgtggtcatgag			

Tm Melting temperature of the amplicon as observed during experimental validations of the primer pairs for real time PCR

[a] For each gene, the first sequence is the upper primer and the second one is the lower; *PADI* peptidylarginine deiminase, *FLG* profilaggrin, *IVL* involucrin, *KRT*10 keratin 10, *LGALS7* galectin 7, *YWHAZ* tyrosine 3/tryptophan 5-monooxygenase activation protein, zeta polypeptide, *B2M* beta-2-microglobulin, *GAPDH* glyceraldehyde-3-phosphate dehydrogenase

[b] *AN* GenBank accession number. For *PADI* genes, the ANs are as follows: *PADI*1, AB033768; *PADI*2, AB030176; *PADI*3, AB026831; *PADI*4, AB017919; *PADI*6, AY422079

PAD activities and auto-deimination assays

Quantification of PAD activity, referred to as the "deimination rate", was performed by western blotting with the anti-citrulline AMC antibody, as described above. To evaluate the activity of PADs in HaCaT and HeLa cells, proteins were extracted into the following buffer [50 mM Tris–HCl pH 7.4, 150 mM NaCl, 1 mM EDTA, 0.5% sodium deoxycholate, 1% Triton X-100 and a 1/100 (v/v) cocktail mammalian protease inhibitors (Sigma-Aldrich)] sonicated on ice for 20 s and centrifuged at 10,000*g* for 10 min at 4°C. After addition of $CaCl_2$ to 10 mM and DTT to 5 mM, the HaCaT and HeLa cell extracts were incubated for 1 h at 50°C, and the proteins immunodetected with the anti-citrulline AMC antibody.

For auto-deimination assays, purified recombinant PAD1–3 were incubated in a first step for 1 h at 37 or 50°C in the following deimination buffer (50 mM Tris–HCl pH 7.4, 10 mM $CaCl_2$, 5 mM DTT). Next, the resulting PAD activity of each isotype was analyzed on a purified recombinant His-filaggrin subunit and revealed by immunodetection using AHF11, as previously described [23].

Statistical analysis

Statistical analyses were performed by unpaired Student's *t* test. All the experiments were done at least three times and the data expressed as the mean ± SEM. Differences were considered significant when the *P* value was less than 0.05.

Topological 3D models of PAD3

As previously described for PAD1 [1], we produced topological 3D models of PAD3 using the atomic coordinates derived from the analysis of PAD4 crystal structures [51]. Schematic ribbon representations of 3D structures of PAD3 were derived from the following PAD4 atomic coordinates available in the Protein Data Bank (http://www.wwpdb.org): Ca^{2+}-free PAD4 (PDB accession code 1WD8, also called "empty model") and PAD4 complexed to Ca^{2+} and benzoyl-L-arginine amide as a substrate (1WDA, also called "full model") [51]. All the 3D modeling structures were produced by the Bioinformatic Tool Server @TOME (@utomatic Threading Optimisation Modeling & Evaluation) at the CBS Informatics Team (http://bioserv.cbs.cnrs.fr/) [52]. They were refined by energy minimization (3,000 iterations) and validated by Ramachandran plot analyses using MSI Insight II modules Biopolymer, CHARMM and Viewer on an O2 SGI workstation and finally analyzed on the "Swiss-Pdb Viewer Deep View 4.0.1 (SPDBV)" [http://www.expasy.org/spdbv/] [53]. After in silico exchanges of arginine (Arg) by citrulline (Cit), the percentages of the accessibility to solvents of the Arg or Cit were evaluate for "empty" and "full" PAD3 models. Distances between the Cγ of Asp-350, the Nδ1 of His-470, the Cγ of Asp-472 and the Sγ of Cys-646, the four major amino acids of the active site, were computed using "SPDBV". From these distances, the volume of the tetrahedrons formed between these four reactive atoms was obtained according to the *Euler* formula [54] (electronic supplementary material, ESM, Fig. S1).

Results

PADs and deimination in human keratinocyte cell lines

Looking for cellular models suitable to test for the regulation of deimination, we first used the immortalized HaCaT keratinocytes, and the cervix adenocarcinoma HeLa cells (data not shown). Even though we detected mRNAs encoding PADs by RT-PCR, and PADs by western blotting, in both cell lines, we were unable to immunodetect deiminated proteins using the anti-citrulline AMC antibody yet were able to detect mono-citrullinated peptides and 100 pg of deiminated filaggrin in the same conditions, as described in "Materials and methods". This suggested that PADs were inactive. Since it is known that a high calcium ion concentration is necessary for PADs to be active, HeLa and HaCaT cells were treated with ionomycin, a calcium-ionophore which increases the calcium influx in the cytoplasm, or with thapsigargin which induces the release of calcium from the endoplasmic reticulum. These treatments did not allow deiminated proteins to be detected (data not shown). These results demonstrate that HeLa and HaCaT keratinocytes are not adapted to analyze endogenous PAD activity and deimination rate. In all the following experiments, we used cultures of primary NHKs, where the expression of *PADI*1–3 has previously been demonstrated.

Vit D increases the PADI1–3 mRNA amounts in NHKs, with distinct kinetics, but not the corresponding proteins

Since the active form of Vit D has been reported to induce PAD activity in human myeloid leukemia HL-60 cells [46] and to promote keratinocyte differentiation [30, 32–34], we investigated the effect of NHK treatment for 24 h with either Vit D (10^{-7} M) or Vit D (10^{-7} M) in presence of 1.5 mM calcium (Vit D + Ca^{2+}). First, we confirmed, by real time PCR, the expression of *PADI*1–3 in NHKs, and the transcriptional effect of Vit D on three keratinocyte differentiation markers, namely the genes of profilaggrin (*FLG*), involucrin (*IVL*), and keratin 10 (*KRT*10) (data not shown). As is the case in the epidermis [19, 20, 22], transcripts of *PADI*4 and 6 were never detected. The Vit D treatment was shown to up-regulate the *PADI*1–3 mRNA amounts and no synergic effect of calcium was observed (Table 2). On the contrary, as previously reported [31, 32, 55], the high calcium concentration potentiated the Vit D-induced over-expression of the differentiation markers by a factor of 2.45 ± 0.58 for *KRT*10, 2.76 ± 1.50 for *FLG*, and 5.88 ± 1.58 for *IVL*. When we analyzed the effect of Vit D over a longer time (Fig. 1), we observed that the three epidermal *PADI* genes showed clearly distinct kinetics of induction: the induction of *PADI*1 and 3 was maximal at 24 h, whereas the quantity of *PADI*2 mRNAs continued to increase until day 10 after the start of the treatment. At day 7, the amount of *PADI*3 transcripts was return to the base line, that of *PADI*1 was slightly, but significantly, increased. At day 21, the Vit D effect on

Table 2 Treatment of NHKs with Vit D increases *PADI*1–3 transcript amounts at 24 h

	*PADI*1	*PADI*2	*PADI*3
Vit D			
a	1.99 ± 0.47	7.96 ± 1.90*	5.25 ± 1.25*
b	1.45 ± 0.30	7.73 ± 0.27**	4.46 ± 0.46*
c	6.45 ± 2.24**	8.87 ± 1.93**	24.69 ± 8.36**
Vit D + Ca^{2+}			
a	2.19 ± 0.45	9.01 ± 1.55*	4.46 ± 1.21*
b	1.52 ± 0.10**	8.02 ± 0.56*	4.04 ± 0.56*
c	4.12 ± 1.63**	8.08 ± 2.09**	16.05 ± 3.94**

Quantitative RT-PCR analysis of the steady-state levels of *PADI*1–3 mRNAs was performed using NHKs treated for 24 h with either 10^{-7} M Vit D in DMSO or DMSO alone (control), and the *YWHAZ* mRNA as the reference. The ratios (treated/control) are expressed as mean ± SEM for three independent experiments (*a–c*), each performed in duplicate plates

*$P < 0.05$, **$P < 0.001$. The *P* values calculated with all the data corresponding to either Vit D or (Vit D + Ca^{2+}) treatments were 2×10^{-4} and 7×10^{-5} for *PADI*1, 3×10^{-13} and 6×10^{-13} for *PADI*2, and 1×10^{-6} and 1×10^{-7} for *PADI*3, respectively

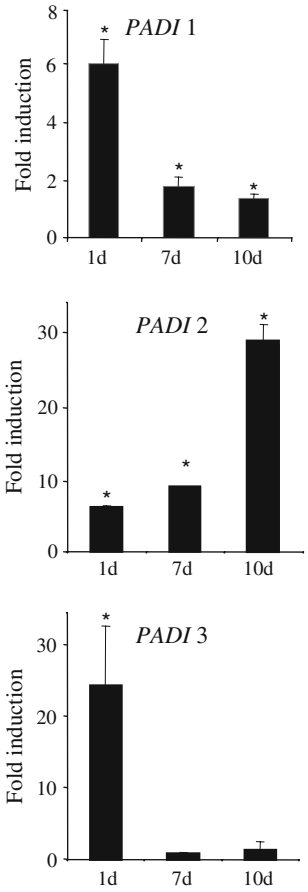

Fig. 1 Effect of Vit D on *PADI*1–3 transcript levels in NHKs at 1, 7, and 10 days. Quantitative RT-PCR analysis of the steady-state levels of *PADI*1–3 mRNAs was performed using NHKs treated for 24 h with either 10^{-7} M Vit D in DMSO or DMSO alone (control), harvested at the indicated time, and using the *YWHAZ* mRNA as the reference to normalize. The ratios (treated/control) are expressed as mean ± SEM for a representative experiment performed in duplicate from among at least three independent experiments (*$P < 0.05$)

*PADI*2 was much less pronounced but continued to be significant, in comparison to DMSO controls, with a measured induction factor of 6.56 ± 0.90. Once, we observed a Vit D effect on the amounts of *PADI*1–3 transcripts after only 6 h of treatment (data not shown). We next investigated the effect of the Vit D treatment on PAD expression at the protein level. Treated NHKs and controls were homogenized in TE-NP40 buffer, a condition known to extract all PADs, and the same amounts of extracted proteins were immunodetected with antibodies against PAD1, PAD2, and PAD3 (Fig. 2a, b). Using actin detection to normalize the data, the amounts of immunodetected PAD1–3 remained unchanged after the Vit D treatments as compared to controls. Since PADs require high calcium concentration to be active (at least in vitro), and Vit D has been reported to increase the intracellular calcium concentration, we also checked the effect of Vit D on the level of PAD activity. To reveal deimination rates, NHK proteins were sequentially extracted in TE-NP40 and Laemmli buffers, and immunodetected with the anti-citrulline AMC antibody (Fig. 2c, d). Within the detection limits of the sensitive AMC antibody, no or very little deimination was detected in the "TE-NP40 extracts" (Fig. 2d, top panels). In contrast, a large smear of deiminated proteins was always observed in the "Laemmli extracts" of NHKs harvested at 6 h, 24 h, or 7 days after the beginning of the treatments (Fig. 2d, bottom panels). Profiles of deiminated proteins were similar between controls and Vit D-treated NHK extracts, and furthermore, after actin normalization, no significant effect on the deimination rate was measured between extracts.

Protein deimination rate in NHKs increases drastically with cell density

Cell density has been largely described as an efficient way to induce differentiation of NHKs [35–37]. We therefore used this model to further analyze the effect of keratinocyte differentiation on PADs. First, by real time PCR, we investigated the state of differentiation of NHKs harvested at low, intermediate, and high cell density. We analyzed the mRNA levels of four differentiation markers, i.e. *KRT*10, *FLG*, and *IVL* as above, and also *galectin* 7 (*LGALS* 7) [41] (Table 3). As expected, the amounts of transcripts of these markers, except *IVL,* were significantly increased at the highest cell density. For *PADI* gene

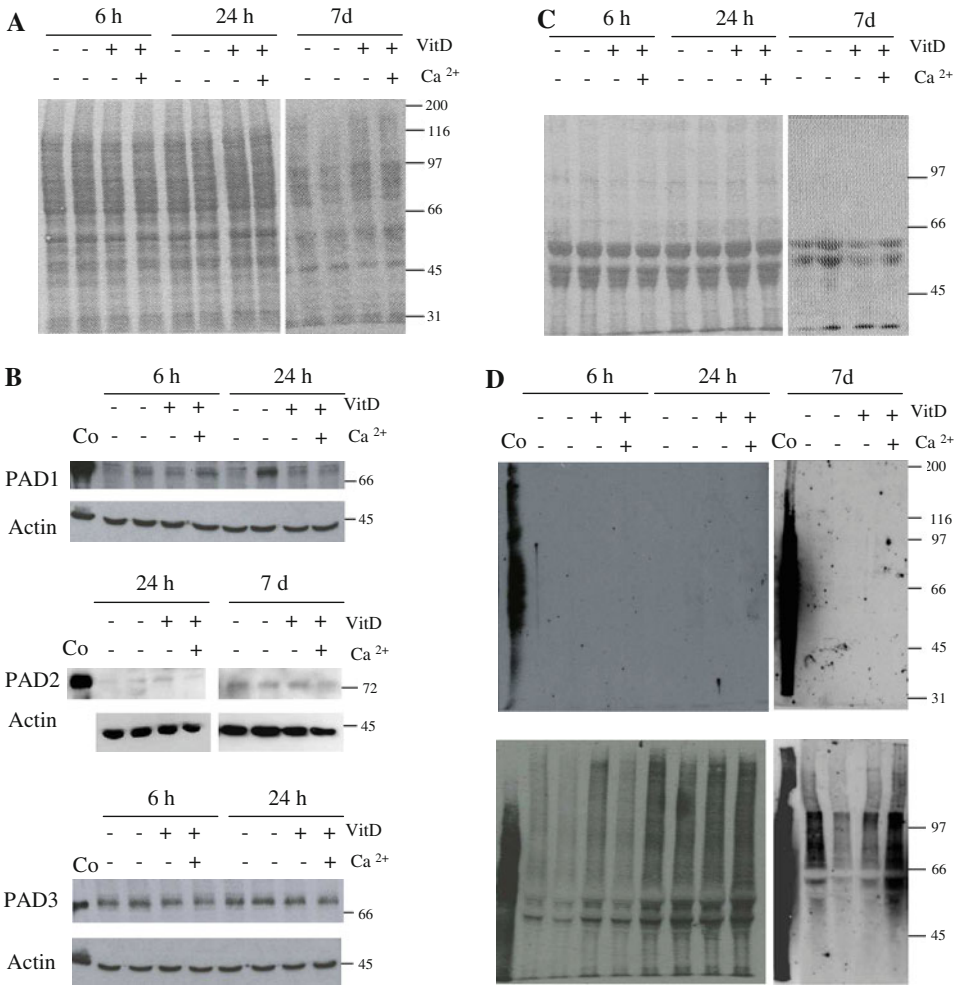

Fig. 2 Effect of Vit D on PAD1–3 protein levels and PAD activity in NHKs. NHKs were treated with Vit D (with or without 1.5 mM calcium) or DMSO as the vehicle, as mentioned on the top of the *panels*, and harvested at the indicated time. **a**,**c** Proteins of the "TE-NP40" (**a**) and "Laemmli" (**c**) extracts were separated by SDS-PAGE, transferred to nitrocellulose membranes and stained with Ponceau S. **b** Immunodetection of PAD1–3 and actin in "TE-NP40" extracts. **d** Immunodetection of deiminated proteins using the anti-citrulline AMC antibody in the "TE-NP40" (*top*) and "Laemmli" (*bottom*) extracts. Molecular masses are reported in kDa on the *right*. Positive controls (*Co*) correspond either to purified recombinant human PAD1, PAD2 and PAD3, and to human epidermal extracts (**b**) or to deiminated fibrinogen (**d**)

expression, the kinetics of induction were distinct. First, the *PADI*3 transcript amount was increased around fivefold at the intermediate cell density and returned to the baseline at the high cell density. Next, as observed for the differentiation marker genes, *PADI*1 transcript level was increased nearly threefold at the high cell density. Finally, the amount of *PADI*2 transcripts remained constant. The high cell density was also efficient to increase PAD protein amounts and to drastically up-regulate PAD activity (Fig. 3). Equal protein amounts of the "TE-NP40 extracts" prepared from NHKs harvested at the intermediate and high cell densities (Fig. 3a, left panel) were immunodetected with the anti-PAD1, -PAD2 and -PAD3 antibodies (Fig. 3b). After actin immunodetection to normalize the data (Fig. 3b, bottom panel) and quantification, the amounts of PAD1 and PAD3 were shown to have risen by a factor of 2.30 ± 0.54 and 3.69 ± 0.41, respectively. In contrast, no effects of NHK cell density on PAD2 protein amounts were observed (1.32 ± 0.02). This was expected since *PADI*2 transcript amounts were not modified. Furthermore, a large increase of the deimination rate was clearly evidenced (by a factor of 12.72 ± 0.93) as shown

Table 3 Modulation of the transcript amounts of differentiation marker and *PADI*1–3 genes by NHK cell density

	NHK cell density	
	Intermediate/low	High/low
*KRT*10	1.04 ± 0.16	8.90 ± 2.28**
FLG	1.02 ± 0.32	7.73 ± 2.57**
IVL	0.40 ± 0.32**	2.61 ± 2.72
LGALS 7	4.56 ± 2.17*	18.09 ± 12.49*
*PADI*1	0.69 ± 0.30*	3.49 ± 0.98**
*PADI*2	1.03 ± 0.34	0.72 ± 0.20*
*PADI*3	5.03 ± 1.62**	0.91 ± 0.19

Quantitative RT-PCR analysis of the steady-state levels of the indicated mRNAs was performed using NHKs harvested at low, intermediate and high cell density, and *YWHAZ* mRNA as the reference. The ratios are expressed as mean ± SEM for three independent experiments, each performed in duplicate plates. Abbreviations are as described in the legend of Table 1

*$P < 0.05$, **$P < 0.001$

when similar protein amounts of the "Laemmli extracts", judged from Ponceau S staining (Fig. 3a, right panel), were immunodetected using the anti-citrulline AMC antibody

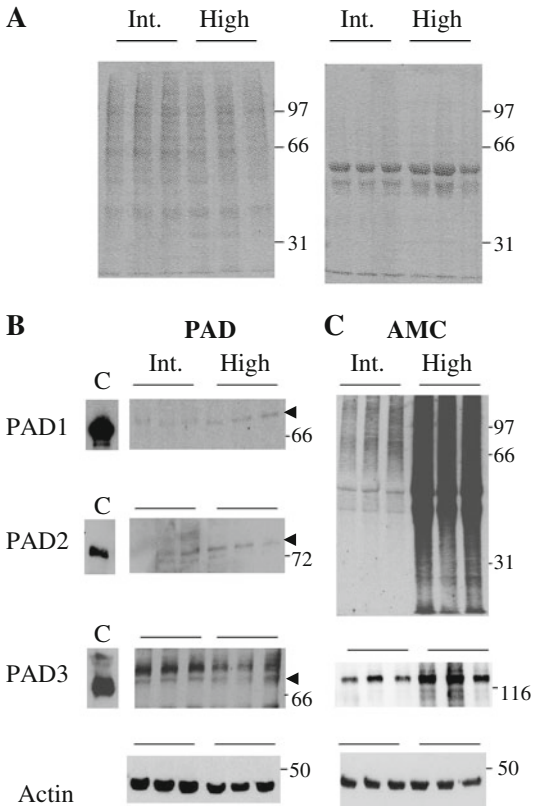

Fig. 3 Effect of cell density on PAD1–3 protein levels and PAD activity. **a** Proteins of the "TE-NP40" (*left panel*) and "Laemmli" (*right panel*) extracts of NHKs harvested at intermediate *(Int.)* and *high* cell density, as mentioned on the *top of the panels*, were stained with Ponceau S. **b** Immunodetections of PAD1–3 (*arrowheads*) and actin in the "TE-NP40" extracts. The positive controls (*c*) correspond to purified human recombinant PAD1 (*top panel*), PAD2 (*middle panel*), and PAD3 (*bottom panel*). **c** Immunodetection in the "Laemmli" extracts of deiminated proteins with the anti-citrulline AMC antibody (*top panel*), of involucrin (*middle panel*), and of actin (*bottom panel*). Data obtained for three independent experiments are shown. Molecular masses are reported in kDa on the *right*

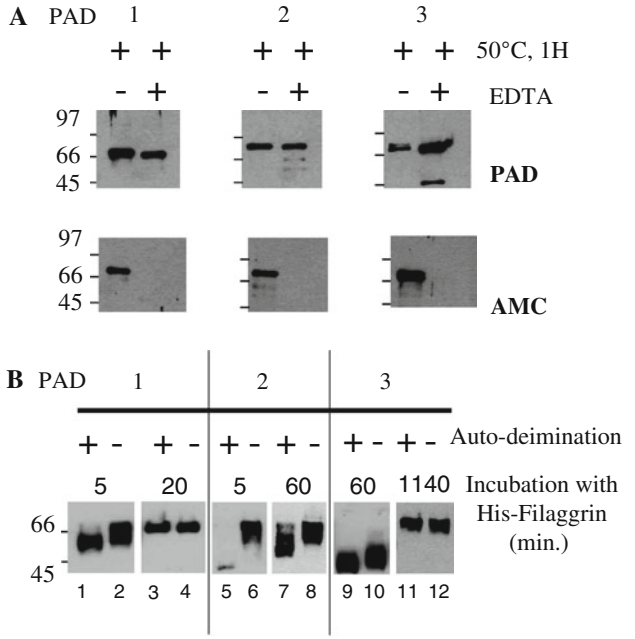

Fig. 4 Calcium-dependent auto-deimination of PAD1–3 modulates their activity. **a** Purified PAD1–3 (as indicated) were incubated in the deimination buffer (Tris–HCl 50 mM pH 7.4, $CaCl_2$ 10 mM, DTT 5 mM) for 1 h at 50°C in the presence (+) or absence (−) of 10 mM EDTA. PAD1–3 were then immunodetected with their respective anti-PAD antibodies (*top panel*) and the anti-citrulline AMC antibody (*bottom panel*). **b** PADs (40 mU) were preincubated for 1 h in the deimination buffer at either 50°C to allow autodeimination (+) or 0°C as a negative control (−). To test for the residual PAD activity after auto-deimination, an equal amount of a recombinant filaggrin subunit was incubated for 5–1,140 min with the preincubated enzymes, as indicated. For each PAD isotype, the times of incubation with filaggrin were chosen according to their efficiency to deiminate this physiological substrate. Filaggrin was then immunodetected with AHF11, a monoclonal antibody recognizing the deiminated filaggrin. Fully deiminated filaggrin is observed at ∼66 kDa, whereas partially deiminated forms migrate between ∼45 and ∼66 kDa. The more efficient the deimination of filaggrin, the closer was its migration to ∼66 kDa

(Fig. 3c). In parallel, involucrin was also increased at the protein level by a factor of 3.09 ± 1.31 (Fig. 3c, middle panel) confirming the effect of cell density on the differentiation of NHKs. To summarize, NHK differentiation, promoted by an increase in cell density, induced larger amounts of *PADI*3 and *PADI*1 mRNAs, of PAD3 and PAD1 proteins and of protein deimination rate. This corresponds to the in vivo situation where PAD3, PAD1 and deiminated filaggrin are detected in the most differentiated keratinocytes.

Auto-deimination might control PAD activity

During in vitro PAD activity measurements, we observed a calcium-dependent auto-deimination of PAD1, 2, and 3, after incubation of the enzymes for 1 h at 50°C, the optimal temperature of PAD activity (Fig. 4a). Similar results were obtained when the enzymes were incubated at 37°C, a more physiological temperature (data not shown). We wondered whether auto-deimination might be another level to control PAD activity. To test this hypothesis, a filaggrin subunit, a physiological substrate of PADs, was incubated for increasing periods of time with the same amount (40 mU) of unmodified (Fig. 4b, lanes −) and auto-deiminated recombinant PAD1, 2 or 3 (Fig. 4b, lanes +; auto-deimination was achieved during 1 h of pre-incubation at 50°C). As we and others have demonstrated previously [8, 23, 47], deimination of filaggrin induced a progressive shift of its migration in SDS-gels, with an apparent molecular mass increasing from ∼45 (non-deiminated) to ∼66 (fully-deiminated) kDa. The more efficient the deimination

of filaggrin, the closer was its migration to ~66 kDa. When filaggrin was incubated with the auto-deiminated PADs, the shift in its migration was generally less pronounced (Fig. 4b, for example compare lanes 1 and 2). Therefore, filaggrin was less deiminated, indicating that the auto-deiminated PADs were less active. This was clearly observed for each isotype at different incubation times according to their kinetics: after 5 min with the auto-deiminated PAD1 (lanes 1 and 2), after 5 and 60 min with the auto-deiminated PAD2 (lanes 5 and 6, and lanes 7 and 8), and after 60 min with the auto-deiminated PAD3 (lanes 9 and 10). When filaggrin was incubated with the auto-deiminated PADs for longer times, it was quite completely deiminated (lanes 3 and 4 for PAD1, lanes 11 and 12 for PAD3, and not shown for PAD2). These data demonstrate that PAD activity is reduced and not completely abolished by their calcium-dependent auto-deimination.

After auto-deimination, we also observed a decrease in the intensity of PAD3 immunodetection in western blotting experiments using the anti-PAD3 anti-peptide antibody (Fig. 4a, top of panel 3). This is probably linked to antigenic variation(s) of the charge and/or structure of the epitopes after deimination and therefore to a reduced avidity of the antibody for its immunogenic peptide (49-DIYISPNMERGRERADTR-66). Assuming a strong structural similarity between PAD3 and PAD4 on the basis of their high sequence similarities, we developed 3D models of PAD3 [without bound-calcium and substrate ("empty" enzyme), with bound-calcium and benzoyl-L-arginine amide as a substrate ("full" enzyme)] from PAD4 crystal structures (see ESM, Fig. S2). According to these models, the four arginyl residues of PAD3 peptide 49–66 are largely accessible to solvents and therefore probably to PAD3 itself for deimination (see ESM, Table S1).

We thought that auto-deimination, inducing a major modification of the global charge of PADs, could change their 3D structure and in turn their activity. To test this hypothesis, we mimic auto-deimination of PAD3 in silico. First, we determined the accessibility to solvents of all the Arg of the enzyme. Then, the most accessible Arg (% of accessibility $\geq$ 40) were replaced by Cit in the 3D models [these new models were refined by energy minimization (3,000 iterations)], and the Arg/Cit accessibility was computed again, as described in the experimental procedures. We also calculated the volumes and surface areas of these 3D structures (of either the entire molecule or the conserved C-terminal domain containing the active site). Unexpectedly, the accessibility to solvents, volumes, and surface areas remained very similar before and after Arg/Cit conversions (see ESM, Tables S1 and S2). In contrast, major differences linked to the presence or absence of both calcium and substrate were observed between PAD3 models. This suggests that the overall framework structure of the enzyme was not drastically perturbed by auto-deimination. Alternatively, auto-deimination might induce subtle conformational changes of the structure and/or accessibility of the active site, sufficient to reduce PAD activity. To test this hypothesis, and according to a multiple alignment analysis of human and murine PAD primary sequences [1], we compared, before and after Arg/Cit substitutions into the PAD3 topological models, the distances between the Asp-350 (atom Cγ), His-470 (atom Nδ1), Asp-472 (atom Cγ), and Cys-646 (atom Sγ) (Fig. 5). These conserved amino acids have been previously described for PAD4 as the four reactive amino acids probably involved directly in the deimination reaction mechanism [51]. After deimination, large increases of distances were observed between the Cγ of Asp-472 and the Sγ of Cys-646 (1.21 Å; 23.54%), the Nδ1 of His-470 (1.3 Å; 38.12%), and the Cγ of Asp-350 (1.42 Å; 19.48%); and also between and the Cγ of Asp-350 and the Sγ of Cys-646 (0.98 Å; 21.40%). This suggested that the volume of the active site of PAD3 increases after auto-deimination. To evaluate this swelling, we calculated the volumes of the tetrahedron form between the four previous atoms of the major amino acids in the active site of the PAD3 topological models. The computed volumes were 64.05 Å^3 for the "empty" PAD3 model, against 11.05 Å^3 for the "full" PAD3 model, confirming the huge effect of calcium binding. More interestingly, substitutions of the accessible Arg by Cit in the "full" 3D model (i.e. the active form) induced an enlargement of 2.34 Å^3 (21.1%) to reach 13.39 Å^3. These larger distances observed between major amino acids involved in the deimination reaction, and consequently the bigger volume of the active site could explain the reduction of PAD activity induced by auto-deimination. Therefore, we could suspect auto-deimination as a major step to regulate deimination in vivo.

Discussion

Since PADs seem to be regulated at multilock points [1, 29], we investigated for the first time the control of deimination during epidermal cell differentiation at several levels. We quantified first the amounts of each *PADI* gene transcript, second the amount of the corresponding PAD isotypes, and third the protein deimination rate as a direct evaluation of PAD activity. Moreover, we tested whether auto-deimination could be an additional level of control.

HeLa and HaCaT cell lines were not suitable for these investigations since no endogenous protein deimination was detectable, even after treatments to increase the intracellular calcium concentration. We therefore used primary NHK cultures, and modulated their differentiation following two in vitro models: (1) treatment with 10^{-7} M Vit D, and (2) high cell density.

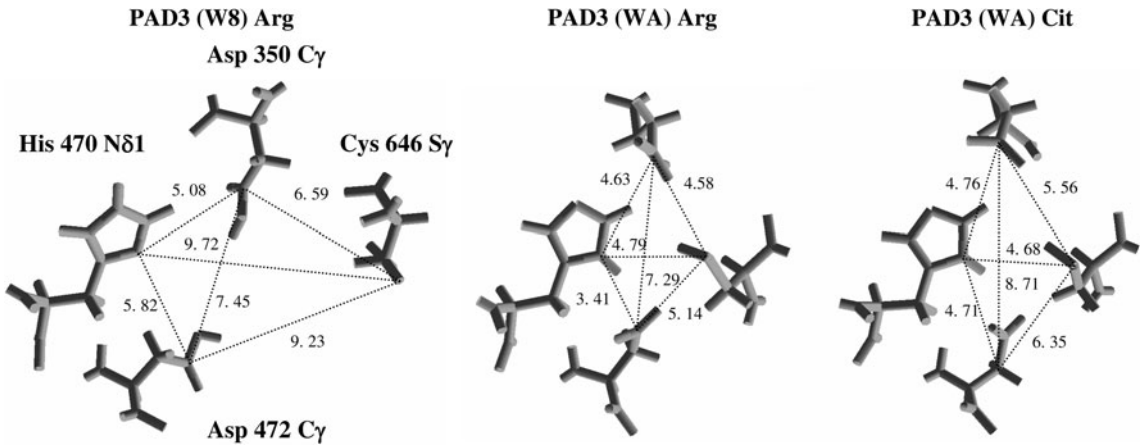

Fig. 5 Auto-deimination induces conformational changes of the PAD3 active site. Zoom, from topological models of PAD3, on the four amino acids (as indicated on the *left panel*) involved during catalysis in the active site: *left panel*, from "empty" PAD3 model (from WD8) with 39 Arg; *middle panel*, from "full" PAD3 model (from WDA) with 39 Arg; *right panel*, from "full" PAD3 model (from WDA) with Cit instead of the most solvent accessible Arg (accessibility $\geq$ 40%). Distances calculated between the atoms of the four major reactive amino acids, as indicated, are reported in Å

In the NHKs, we showed that the amounts of *PADI*1–3 gene transcripts are up-regulated as early as 6–24 h after starting Vit D treatment. Moreover, for the first time, we demonstrated by a quantitative RT-PCR approach that the three *PADI* genes follow distinct kinetics of regulation during differentiation of NHKs induced by Vit D. Whereas the amounts of *PADI*3 rapidly return to the baseline, the effect on *PADI*1 is still observable at day 10 after the beginning of the treatment, and the amount of *PADI*2 transcript continues to increase until day 10. The differentiation of NHKs induced by high cell density controls the amounts of the *PADI* gene transcripts differently. In this cellular model, *PADI*2 is not affected whereas *PADI*1 and *PADI*3 are clearly up-regulated. In summary, the three epidermal *PADI* genes are controlled differentially during the keratinocyte differentiation program. In agreement with this hypothesis, we have already demonstrated, using NHKs exposed to high calcium concentration (1.5 mM), another model to induce differentiation, that the minimal promoter-driven transcription of *PADI*3 but not *PADI*2 is strongly increased through chromatin looping events by the binding of AP-1 factors to several long-range enhancers, 86 kb and 81–82 kb distant from the *PADI*3 promoter [27, 28]. During the course of this present work, transcriptional profiling of Vit D-treated immortalized (KerTr) and primary NHKs using Affymetrix genechips and Q-PCR has confirmed the up-regulation of *PADI*1–3 and other differentiation-related genes [56]. However, in this latter study, the corresponding protein levels and enzymatic activities have not been investigated. Moreover, the authors have proposed that a Vit D treatment could be therapeutically relevant in psoriasis to correct the deimination alterations observed in the patient epidermis. Our own results do not sustain this proposal since inducing the mRNA levels is not sufficient to induce the protein level and deimination.

To further investigate the Vit D up-regulation of *PADI*1–3 genes in NHKs, we performed luciferase-reporter assays as previously described [28]. NHKs, cultured in a medium containing low or high amounts of calcium, with (10^{-7} M) or without Vit D, were transfected with reporter plasmids containing 700-bp segments upstream of the transcription initiation start site as *PADI*1–3 promoters or corresponding controls. However, no effects of the Vit D treatment were observed, suggesting that Vit D does not act through Vit D response elements (VDRE) located in the *PADI*1–3 minimal promoters (data not shown). Through the use of transgenic murine models, the Vit D receptor (VDR) has recently been demonstrated to be involved in hair follicle differentiation and in β-catenin-induced skin tumors [57]. A *Padi*3 two- to fourfold transcriptional up-regulation was induced by treatment, with the Vit D analog EB1089, of primary keratinocytes from wild-type mice but not VDR null mice. In the same study using chromatin immunoprecipitation experiments, 3 functional variant consensus VDREs were identified among 11 putative ones upstream of the *Padi*3 promoter, in the distal region between nucleotides −2,839 and −3,095. Based on these data and, using the "NHR scan program" (http://www.cisreg.ca/cgi-bin/NHR-scan/nhr_scan.cgi), we found at least 11 canonical direct repeats (DR1 to 5) in the 6,000 bp upstream of the human *PADI*3 transcription initiation start site (Genbank accession number AJ549502) (data not shown). Some of them could be functional. Finally, to test for the in vivo necessity of Vit D, for Pad expression in the skin, we immunodetected Pad1 and 3 on sections of formalin-fixed skin from adult wild-type and VDR null mice. In the epidermis, we did not detect

any obvious differences in the location or any decrease in the expression level of either of these isotypes (see ESM, Fig. S3). This suggests that the expression of Pad1 and 3 in basal conditions does not need Vit D stimulation via the VDR pathway.

In this work, we also observed for the first time that PADs are regulated in NHKs at the post-transcriptional level. Indeed, in spite of the up-regulation of mRNAs encoding PAD1–3, the corresponding proteins are not over-expressed and the deimination rate is not increased in Vit D-treated NHKs compared to controls (note that 0.1% DMSO induces deimination by itself). Such a complex PAD regulation during differentiation has been previously observed in other cellular models. For example, during monocyte/macrophage differentiation, *PADI*2 and *PADI*4 mRNA amounts are unrelated to PAD2 and PAD4 protein levels [38]. It has been suggested that *PADI*2 mRNA translation is subject to differentiation stage-specific regulation by its 3′ untranslated terminal region, but other mechanisms may be proposed, including messenger regulation by miRNAs. Using HeLa and HaCaT cells, we also highlight the fact that PADs could be expressed but not active. At least one PAD isoform was detected in both cell lines without any deiminated proteins. Interestingly, in normal epidermis, PAD1 and PAD2 are expressed in the basal and spinous layers, where deiminated proteins are not detected. This strongly suggests that PADs are also controlled in vivo at the level of their enzymatic activity. One way to achieve this level of control may be a post-translational modification. We give here the first evidence that in vitro auto-deimination reduces the activity of PAD1–3, suggesting that auto-deimination could be a new step of PAD regulation in vivo, as auto-phosphorylation is for kinases. Auto-regulation of PADs by deimination could control the deimination rate of filaggrin and therefore have major incidences on its metabolism and consequently on *stratum corneum* moisturizing and barrier functions. To optimize the in vitro auto-deimination, we incubated the enzymes at 50°C in the presence of DTT, the conditions where the PAD activity is known to be maximal. Similar results were obtained at 37°C. In addition, since we have previously shown [23] that deimination of filaggrin is highly effective at 22°C, the mean temperature of the external layer of the epidermis, we suspect that auto-deimination could also occur in these conditions. The existence of auto-deimination of PADs in vivo remains to be proved, and the citrullination sites to be identify. These ongoing experiments will help to understand the exact mechanisms involved in the control of PAD activity, at the molecular levels. Unfortunately, point mutation assays to mimic the effects of citrullination on the recombinant enzymes are not possible since citrulline is not a naturally encoded amino acid. It should also be noticed that auto-deimination of PADs does not seem to induce large conformational changes of the enzymes, as suggested by our computational modeling of PAD3 structure. In contrast, we propose that subtle changes (increasing distances between major amino acids involved in the catalytic reaction, and increasing volume) at the level of the active site could be sufficient to reduce (not abolish) the catalytic PAD activities. This modeling does not take into account a putative effect of DTT on PAD disulfide bridges, but the enzyme activity is known to be enhanced in the presence of DTT and inhibited by treatment with monoiodoacetate, supporting the conclusions that PADs require free SH for activity. In agreement, no disulfide bridge between cysteines was observed in the structure of PAD4 deduced from cristallographic data [51] and the deduced model of PAD1 and 3 [1, our present work].

Furthermore, this work demonstrates, for the first time, that NHK cell density enhances the transcription of the human *PADI*3 (fivefold) and *PADI*1 (threefold) genes, the expression of PAD3 and PAD1, and mainly the deimination rate of cellular proteins (by a factor of 12). This expands the list of epidermal differentiation markers, including filaggrin, keratins, involucrin, and galectins, regulated by cell confluence.

The expression of PAD4 in HeLa and HaCaT cells and its absence in NHKs could be related to the fact that these cell lines are malignant or transformed. In agreement with this hypothesis, PAD4 has been detected in various carcinomas (especially adenocarcinomas) but not in the corresponding normal tissues [58]. Furthermore, overexpression of PAD4 has been associated with G1-phase cell arrest and apoptosis events in hematopoietic cells [59, 60].

The regulation (or disregulation) of PADs in dry skin environments such as atopic dermatitis, the prevalence of which increases in children of industrial countries [61], and in other pathological situations such as rheumatoid arthritis, is currently being deciphered in our research unit.

Acknowledgments We thank C. Pons for her excellent technical assistance, the staff of the "Laboratoire de Biologie Cellulaire Cutanée du CERPER", especially I. Cerutti, M. J. Haure and S. Julié, for their technical advice, the sequencing and genotyping facility of the IFR150 at Toulouse-Purpan, particularly C. Offer and H. Brun for their precious high efficiency, and the histological facility at Toulouse-Purpan, especially F. Capilla for her technical advice. We are indebted to Dr A Ishigami (Chiba, Japan) for the anti-PAD2 antibody and to Drs H Palmer and G. Carmeliet (Cancer Research UK Cambridge Research Institute, Cambridge, UK) for providing us with skin sections of VDR-null mice and control littermates. We would also particularly like to thank N. Mattiuzzo for his technical bioinformatics suggestions for performing VDRE sequences analysis, and Drs M. Sebbag and C.-Y. Hsu for their advice and helpful discussions. This work was supported by grants from the "Centre National de la Recherche Scientifique" (CNRS), the "Société Française de Dermatologie" and the "Centre Européen de Recherche sur la Peau et les Epithéliums de Revêtement" (CERPER, Toulouse, France) and by the "Institut National de la Santé et de la Recherche Médicale" (INSERM).

References

1. Méchin MC, Sebbag M, Arnaud J, Nachat R, Foulquier C, Adoue V, Coudane F, Duplan H, Schmitt AM, Chavanas S, Guerrin M, Serre G, Simon M (2007) Update on peptidylarginine deiminases and deimination in skin physiology and severe human diseases. Int J Cosmet Sci 29:147–168
2. Sebbag M, Chapuy-Regaud S, Auger I, Petit-Texeira E, Clavel C, Nogueira L, Vincent C, Cornelis F, Roudier J, Serre G (2004) Clinical and pathophysiological significance of the autoimmune response to citrullinated proteins in rheumatoid arthritis. Joint Bone Spine 71:493–502
3. Harauz G, Musse AA (2007) A tale of two citrullines—structural and functional aspects of myelin basic protein deimination in health and disease. Neurochem Res 32:137–158
4. Jones JE, Causey CP, Knuckley B, Slack-Noyes JL, Thompson PR (2009) Protein arginine deiminase 4 (PAD4): current understanding and future therapeutic potential. Curr Opin Drug Discov Devel 12:616–627
5. Senshu T, Kan S, Ogawa H, Manabe M, Asaga H (1996) Preferential deimination of keratin K1 and filaggrin during the terminal differentiation of human epidermis. Biochem Biophys Res Commun 225:712–719
6. Rogers GE, Taylor LD (1977) The enzymic derivation of citrulline residues from arginine residues in situ during the biosynthesis of hair proteins that are cross-linked by isopeptide bonds. Adv Exp Med Biol 86A:283–294
7. Tarcsa E, Marekov LN, Andreoli J, Idler WW, Candi E, Chung SI, Steinert PM (1997) The fate of trichohyalin. Sequential post-translational modifications by peptidyl-arginine deiminase and transglutaminases. J Biol Chem 272:27893–27901
8. Tarcsa E, Marekov LN, Mei G, Melino G, Lee SC, Steinert PM (1996) Protein unfolding by peptidylarginine deiminase. Substrate specificity and structural relationships of the natural substrates trichohyalin and filaggrin. J Biol Chem 271:30709–30716
9. Kizawa K, Takahara H, Troxler H, Kleinert P, Mochida U, Heizmann CW (2008) Specific citrullination causes assembly of a globular S100A3 homotetramer: a putative Ca^{2+} modulator matures human hair cuticle. J Biol Chem 283:5004–5013
10. Rawlings AV, Harding CR (2004) Moisturization and skin barrier function. Dermatol Ther 17(Suppl 1):43–48
11. Smith FJ, Irvine AD, Terron-Kwiatkowski A, Sandilands A, Campbell LE, Zhao Y, Liao H, Evans AT, Goudie DR, Lewis-Jones S, Arseculeratne G, Munro CS, Sergeant A, O'Regan G, Bale SJ, Compton JG, DiGiovanna JJ, Presland RB, Fleckman P, McLean WH (2006) Loss-of-function mutations in the gene encoding filaggrin cause ichthyosis vulgaris. Nat Genet 38:337–342
12. Palmer CN, Irvine AD, Terron-Kwiatkowski A, Zhao Y, Liao H, Lee SP, Goudie DR, Sandilands A, Campbell LE, Smith FJ, O'Regan GM, Watson RM, Cecil JE, Bale SJ, Compton JG, DiGiovanna JJ, Fleckman P, Lewis-Jones S, Arseculeratne G, Sergeant A, Munro CS, El Houate B, McElreavey K, Halkjaer LB, Bisgaard H, Mukhopadhyay S, McLean WH (2006) Common loss-of-function variants of the epidermal barrier protein filaggrin are a major predisposing factor for atopic dermatitis. Nat Genet 38:441–446
13. McGrath JA (2008) Filaggrin and the great epidermal barrier grief. Australas J Dermatol 49:67–73 quiz 73-4
14. Howell MD, Fairchild HR, Kim BE, Bin L, Boguniewicz M, Redzic JS, Hansen KC, Leung DY (2008) Th2 cytokines act on S100/A11 to downregulate keratinocyte differentiation. J Investig Dermatol 128:2248–2258
15. Howell MD, Kim BE, Gao P, Grant AV, Boguniewicz M, Debenedetto A, Schneider L, Beck LA, Barnes KC, Leung DY (2007) Cytokine modulation of atopic dermatitis filaggrin skin expression. J Allergy Clin Immunol 120:150–155
16. Kamata Y, Taniguchi A, Yamamoto M, Nomura J, Ishihara K, Takahara H, Hibino T, Takeda A (2009) Neutral cysteine protease bleomycin hydrolase is essential for the breakdown of deiminated filaggrin into amino acids. J Biol Chem 284:12829–12836
17. Ishida-Yamamoto A, Senshu T, Eady RA, Takahashi H, Shimizu H, Akiyama M, Iizuka H (2002) Sequential reorganization of cornified cell keratin filaments involving filaggrin-mediated compaction and keratin 1 deimination. J Investig Dermatol 118:282–287
18. Ishida-Yamamoto A, Senshu T, Takahashi H, Akiyama K, Nomura K, Iizuka H (2000) Decreased deiminated keratin K1 in psoriatic hyperproliferative epidermis. J Investig Dermatol 114:701–705
19. Chavanas S, Méchin MC, Takahara H, Kawada A, Nachat R, Serre G, Simon M (2004) Comparative analysis of the mouse and human peptidylarginine deiminase gene clusters reveals highly conserved non-coding segments and a new human gene, PADI6. Gene 330:19–27
20. Guerrin M, Ishigami A, Méchin MC, Nachat R, Valmary S, Sebbag M, Simon M, Senshu T, Serre G (2003) cDNA cloning, gene organization and expression analysis of human peptidylarginine deiminase type I. Biochem J 370:167–174
21. Nachat R, Méchin MC, Charveron M, Serre G, Constans J, Simon M (2005) Peptidylarginine deiminase isoforms are differentially expressed in the anagen hair follicles and other human skin appendages. J Investig Dermatol 125:34–41
22. Nachat R, Méchin MC, Takahara H, Chavanas S, Charveron M, Serre G, Simon M (2005) Peptidylarginine deiminase isoforms 1–3 are expressed in the epidermis and involved in the deimination of K1 and filaggrin. J Investig Dermatol 124:384–393
23. Méchin MC, Enji M, Nachat R, Chavanas S, Charveron M, Ishida-Yamamoto A, Serre G, Takahara H, Simon M (2005) The peptidylarginine deiminases expressed in human epidermis differ in their substrate specificities and subcellular locations. Cell Mol Life Sci 62:1984–1995
24. Dong S, Kanno T, Yamaki A, Kojima T, Shiraiwa M, Kawada A, Méchin MC, Chavanas S, Serre G, Simon M, Takahara H (2006) NF-Y and Sp1/Sp3 are involved in the transcriptional regulation of the peptidylarginine deiminase type III gene (PADI3) in human keratinocytes. Biochem J 397:449–459
25. Dong S, Kojima T, Shiraiwa M, Méchin MC, Chavanas S, Serre G, Simon M, Kawada A, Takahara H (2005) Regulation of the expression of peptidylarginine deiminase type II gene (PADI2) in human keratinocytes involves Sp1 and Sp3 transcription factors. J Investig Dermatol 124:1026–1033
26. Dong S, Ying S, Kojima T, Shiraiwa M, Kawada A, Méchin MC, Adoue V, Chavanas S, Serre G, Simon M, Takahara H (2008) Crucial roles of MZF1 and Sp1 in the transcriptional regulation of the peptidylarginine deiminase type I gene (PADI1) in human keratinocytes. J Investig Dermatol 128:549–557
27. Chavanas S, Adoue V, Méchin MC, Ying S, Dong S, Duplan H, Charveron M, Takahara H, Serre G, Simon M (2008) Long-range enhancer associated with chromatin looping allows AP-1 regulation of the peptidylarginine deiminase 3 gene in differentiated keratinocyte. PLoS ONE 3:e3408. doi:10.1371/journal.pone.0003408
28. Adoue V, Chavanas S, Coudane F, Méchin MC, Caubet C, Ying S, Dong S, Duplan H, Charveron M, Takahara H, Serre G, Simon M (2008) Long-range enhancer differentially regulated by c-Jun and JunD controls peptidylarginine deiminase-3 gene in keratinocytes. J Mol Biol 384:1048–1057
29. Ying S, Dong S, Kawada A, Kojima T, Chavanas S, Méchin MC, Adoue V, Serre G, Simon M, Takahara H (2009) Transcriptional

regulation of peptidylarginine deiminase expression in human keratinocytes. J Dermatol Sci 53:2–9
30. Hosomi J, Hosoi J, Abe E, Suda T, Kuroki T (1983) Regulation of terminal differentiation of cultured mouse epidermal cells by 1 alpha, 25-dihydroxyvitamin D3. Endocrinology 113:1950–1957
31. Bikle DD, Oda Y, Xie Z (2004) Calcium and 1, 25(OH)2D: interacting drivers of epidermal differentiation. J Steroid Biochem Mol Biol 89–90:355–360
32. Bikle DD, Pillai S (1993) Vitamin D, calcium, and epidermal differentiation. Endocr Rev 14:3–19
33. Reichrath J (2007) Vitamin D and the skin: an ancient friend, revisited. Exp Dermatol 16:618–625
34. Reichrath J, Lehmann B, Carlberg C, Varani J, Zouboulis CC (2007) Vitamins as hormones. Horm Metab Res 39:71–84
35. Poumay Y, Herphelin F, Smits P, De Potter IY, Pittelkow MR (1999) High-cell-density phorbol ester and retinoic acid upregulate involucrin and downregulate suprabasal keratin 10 in autocrine cultures of human epidermal keratinocytes. Mol Cell Biol Res Commun 2:138–144
36. Poumay Y, Pittelkow MR (1995) Cell density and culture factors regulate keratinocyte commitment to differentiation and expression of suprabasal K1/K10 keratins. J Investig Dermatol 104:271–276
37. Nilsson JA, Hedberg JJ, Vondracek M, Staab CA, Hansson A, Hoog JO, Grafstrom RC (2004) Alcohol dehydrogenase 3 transcription associates with proliferation of human oral keratinocytes. Cell Mol Life Sci 61:610–617
38. Vossenaar ER, Radstake TR, van der Heijden A, van Mansum MA, Dieteren C, de Rooij DJ, Barrera P, Zendman AJ, van Venrooij WJ (2004) Expression and activity of citrullinating peptidylarginine deiminase enzymes in monocytes and macrophages. Ann Rheum Dis 63:373–381
39. Suzuki A, Yamada R, Chang X, Tokuhiro S, Sawada T, Suzuki M, Nagasaki M, Nakayama-Hamada M, Kawaida R, Ono M, Ohtsuki M, Furukawa H, Yoshino S, Yukioka M, Tohma S, Matsubara T, Wakitani S, Teshima R, Nishioka Y, Sekine A, Iida A, Takahashi A, Tsunoda T, Nakamura Y, Yamamoto K (2003) Functional haplotypes of PADI4, encoding citrullinating enzyme peptidylarginine deiminase 4, are associated with rheumatoid arthritis. Nat Genet 34:395–402
40. Rheinwald JG, Green H (1975) Serial cultivation of strains of human epidermal keratinocytes: the formation of keratinizing colonies from single cells. Cell 6:331–343
41. Sarafian V, Jans R, Poumay Y (2006) Expression of lysosome-associated membrane protein 1 (Lamp-1) and galectins in human keratinocytes is regulated by differentiation. Arch Dermatol Res 298(2):73–81
42. Foulquier C, Sebbag M, Clavel C, Chapuy-Regaud S, Al Badine R, Méchin MC, Vincent C, Nachat R, Yamada M, Takahara H, Simon M, Guerrin M, Serre G (2007) Peptidyl arginine deiminase type 2 (PAD-2) and PAD-4 but not PAD-1, PAD-3, and PAD-6 are expressed in rheumatoid arthritis synovium in close association with tissue inflammation. Arthritis Rheum 56:3541–3553
43. Wright PW, Bolling LC, Calvert ME, Sarmento OF, Berkeley EV, Shea MC, Hao Z, Jayes FC, Bush LA, Shetty J, Shore AN, Reddi PP, Tung KS, Samy E, Allietta MM, Sherman NE, Herr JC, Coonrod SA (2003) ePAD, an oocyte and early embryo-abundant peptidylarginine deiminase-like protein that localizes to egg cytoplasmic sheets. Dev Biol 256:73–88
44. Senshu T, Akiyama K, Kan S, Asaga H, Ishigami A, Manabe M (1995) Detection of deiminated proteins in rat skin: probing with a monospecific antibody after modification of citrulline residues. J Investig Dermatol 105:163–169
45. Shimada N, Handa S, Uchida Y, Fukuda M, Maruyama N, Asaga H, Choi EK, Lee J, Ishigami A (2009) Developmental and age-related changes of peptidylarginine deiminase 2 in the mouse brain. J Neurosci Res. doi:10.1002/jnr.22255
46. Nakashima K, Hagiwara T, Ishigami A, Nagata S, Asaga H, Kuramoto M, Senshu T, Yamada M (1999) Molecular characterization of peptidylarginine deiminase in HL-60 cells induced by retinoic acid and 1alpha, 25-dihydroxyvitamin D(3). J Biol Chem 274:27786–27792
47. Kanno T, Kawada A, Yamanouchi J, Yosida-Noro C, Yoshiki A, Shiraiwa M, Kusakabe M, Manabe M, Tezuka T, Takahara H (2000) Human peptidylarginine deiminase type III: molecular cloning and nucleotide sequence of the cDNA, properties of the recombinant enzyme, and immunohistochemical localization in human skin. J Investig Dermatol 115:813–823
48. Girbal-Neuhauser E, Durieux JJ, Arnaud M, Dalbon P, Sebbag M, Vincent C, Simon M, Senshu T, Masson-Bessière C, Jolivet-Reynaud C, Jolivet M, Serre G (1999) The epitopes targeted by the rheumatoid arthritis-associated antifilaggrin autoantibodies are posttranslationally generated on various sites of (pro)filaggrin by deimination of arginine residues. J Immunol 162:585–594
49. Rozen S, Skaletsky H (2000) Primer3 on the WWW for general users and for biologist programmers. Methods Mol Biol 132:365–386
50. Vandesompele J, De Preter K, Pattyn F, Poppe B, Van Roy N, De Paepe A, Speleman F (2002) Accurate normalization of real-time quantitative RT-PCR data by geometric averaging of multiple internal control genes. Genome Biol 3. RESEARCH0034
51. Arita K, Hashimoto H, Shimizu T, Nakashima K, Yamada M, Sato M (2004) Structural basis for Ca(2+)-induced activation of human PAD4. Nat Struct Mol Biol 11:777–783
52. Douguet D, Labesse G (2001) Easier threading through web-based comparisons and cross-validations. Bioinformatics 17:752–753
53. Guex N, Peitsch MC (1997) Swiss-model and the Swiss-Pdb viewer: an environment for comparative protein modeling. Electrophoresis 18:2714–2723
54. Dove KL, Summer JS (1992) Tetrahedra with integer edges and interger volume. Math Mag 65:104–111
55. Bikle DD, Chang S, Crumrine D, Elalieh H, Man MQ, Dardenne O, Xie Z, Arnaud RS, Feingold K, Elias PM (2004) Mice lacking 25OHD 1alpha-hydroxylase demonstrate decreased epidermal differentiation and barrier function. J Steroid Biochem Mol Biol 89–90:347–353
56. Lu J, Goldstein KM, Chen P, Huang S, Gelbert LM, Nagpal S (2005) Transcriptional profiling of keratinocytes reveals a vitamin D-regulated epidermal differentiation network. J Investig Dermatol 124:778–785
57. Palmer HG, Anjos-Afonso F, Carmeliet G, Takeda H, Watt FM (2008) The vitamin D receptor is a Wnt effector that controls hair follicle differentiation and specifies tumor type in adult epidermis. PLoS ONE 3:e1483. doi:10.1371/journal.pone.0001483
58. Chang X, Han J (2006) Expression of peptidylarginine deiminase type 4 (PAD4) in various tumors. Mol Carcinog 45:183–196
59. Liu GY, Liao YF, Chang WH, Liu CC, Hsieh MC, Hsu PC, Tsay GJ, Hung HC (2006) Overexpression of peptidylarginine deiminase IV features in apoptosis of haematopoietic cells. Apoptosis 11:183–196
60. Yao H, Li P, Venters BJ, Zheng S, Thompson PR, Pugh BF, Wang Y (2008) Histone Arg modifications and p53 regulate the expression of OKL38, a mediator of apoptosis. J Biol Chem 283:20060–20068
61. de Benedictis FM, Franceschini F, Hill D, Naspitz C, Simons FE, Wahn U, Warner JO, de Longueville M (2009) The allergic sensitization in infants with atopic eczema from different countries. Allergy 64:295–303